Geosci. Instrum. Method. Data Syst. Discuss., 5, 385–404, 2015
www.geosci-instrum-method-data-syst-discuss.net/5/385/2015/
doi:10.5194/gid-5-385-2015


Geoscientific Instrumentation Methods and Data Systems Discussions
Open Access
EGU



# Sodankylä ionospheric tomography dataset 2003–2014

**J. Norberg[1], L. Roininen[2,3], A. Kero[3], T. Raita[3], T. Ulich[3], M. Markkanen[4], L. Juusola[1], and K. Kauristie[1]**

[1]Finnish Meteorological Institute, Helsinki, Finland
[2]Department of Mathematics, Tallinn University of Technology, Tallinn, Estonia
[3]Sodankylä Geophysical Observatory, University of Oulu, Sodankylä, Finland
[4]Eigenor Corporation, Sodankylä, Finland

Received: 16 November 2015 – Accepted: 23 November 2015 – Published: 4 December 2015

Correspondence to: J. Norberg (johannes.norberg@fmi.fi)

Published by Copernicus Publications on behalf of the European Geosciences Union.







## Abstract

Sodankylä Geophysical Observatory has been operating a tomographic receiver network and collecting the produced data since 2003. The collected dataset consists of phase difference curves measured from Russian COSMOS dual-frequency (150/400 MHz) low-Earth-orbit satellite signals, and tomographic electron density reconstructions obtained from these measurements. In this study vertical total electron content (VTEC) values are integrated from the reconstructed electron densities to make a qualitative and quantitative analysis to validate the long-term performance of the tomographic system. During the observation period, 2003–2014, there were three-to-five operational stations at the Fenno-Scandinavian sector. Altogether the analysis consists of around 66 000 overflights, but to ensure the quality of the reconstructions, the examination is limited to cases with descending (north to south) overflights and maximum elevation over 60°. These constraints limit the number of overflights to around 10 000. Based on this dataset, one solar cycle of ionospheric vertical total electron content estimates is constructed. The measurements are compared against International Reference Ionosphere IRI-2012 model, F10.7 solar flux index and sunspot number data. Qualitatively the tomographic VTEC estimate corresponds to reference data very well, but the IRI-2012 model are on average 40 % higher of that of the tomographic results.

## 1 Introduction

The use of tomographic methods for ionospheric research was first suggested by Austen et al. (1988). In ionospheric tomography with low Earth orbit (LEO) satellites, the objective is to reconstruct the ionospheric electron density in a two, three or four-dimensional domain from ground-based measurements of beacon satellite radio signals. The measured quantity is the phase shift of the transmitted radio signal. The phase shift is proportional to the number density of free electrons along the signal path, hence the measurements can be modeled as line integrals of ionospheric





GID
5, 385–404, 2015



electron density. This results in a limited angle tomography inverse problem, which requires some regularization scheme to stabilize the ill-posedness of the problem. The method operated by Sodankylä Geophysical Observatory (SGO), is carried out within the framework of Bayesian statistical inverse problems. The current method is reported by Markkanen et al. (1995). Stabilization of the inverse problem is given with first order difference priors with a Chapman-profile used in weighting the variances in the altitude. In a more recent analysis development, similar framework has been used with Gaussian Markov random field approximations for proper prior covariance structures (Norberg et al., 2015). Bust and Mitchell (2008) provide a good overview on other commonly used methods and on overall development of the topic.

SGO has been producing ionospheric tomography measurements operationally since 2003. For the observation period 2003–2014, the dataset consists around one solar cycle of measurements. SGO's measurements are based on Russian polar orbiting COSMOS satellites equipped with dual-frequency 150/400 MHz beacon transmitters. The geographical locations of the SGO chain are plotted in black triangles in Fig. 1. Recently Finnish Meteorological Institute (FMI), in collaboration with SGO, has installed six additional stations in the region allowing the observation area to expand from Tartu, Estonia to Longyearbyen, Svalbard, Norway, shown as black circles in Fig. 1. These TomoScand stations are able to receive signals from any beacon satellite transmitting at dual-frequency 150/400 MHz (Vierinen et al., 2014). For example the CASSIOPE/e-POP satellite mission has provided one new transmitter. A similar chain, operated by Polar Geophysical Institute, is on the Kolan peninsula and Karelia in North-West Russia (Kunitsyn and Tereshchenko, 2003). In this specific study, the SGO receiver chain and COSMOS satellites are considered.

The lack of horizontal measurements in ionospheric tomography causes well known problems to reconstructions, especially when steep vertical gradients are involved. However, it was reported by Nygrén et al. (1996) that in the SGO's algorithm, the local overestimations are usually compensated with local underestimations elsewhere, and vice versa; e.g. overestimation in layer thickness leads to reduced peak density. Hence,





GID
5, 385–404, 2015



the solution for the absolute level, i.e. the total electron content (TEC) of relative electron density measurements is more stabile than the actual profiles, and can be well estimated within the inversion. To characterize the long-term trends in ionosphere the TEC measurements are integrated vertically (VTEC) over each receiver station. Compressing the data to an ionospheric VTEC value results in more robust statistic and allows more straightforward visualization.

Typical choices for VTEC validation are GPS measurements. These methods are well-established, but they do not measure directly the high-latitude ionosphere, as the satellites are not on polar-orbiting tracks, i.e. they remain too south for reliable direct measurements. Moreover, the GPS altitude is so high that the measurements include also almost the entire plasmasphere. Especially at night time the plasmaspheric contribution to electron density can be significant. Jee et al. (2014) have performed similar studies for the last two solar minimum periods with TOPEX and JASON-1 satellites with orbital altitudes of 1337 km and inclination of 66.038°. From these satellites the VTEC can be solved as a by-product of altimetry estimation, but only over global ocean.

The specific objective of this paper, is to investigate the solar cycle variations in VTEC data obtained from the ionospheric tomography analysis. As reference material, the VTEC values derived from the IRI-2012 model (Bilitza et al., 2014), F10.7 solar flux index and sunspot number data are used. By quantifying first the solar cycle variations in data, the opportunities to use similar data also in studies on slower trends in high-latitude VTEC values can be considered. Based on model predictions, increased levels of carbon dioxide and methane are predicted to cool the thermosphere, and hence lower the so-called F2-peak layer, see e.g. Roble and Dickinson (1989). Indirect measurements of the height $hmF2$ of the ionospheric F2 peak have been studied by a number of authors, see e.g. Bremer (1992, 1998); Ulich and Turunen (1997); Upadhyay and Mahajan (1998); Cnossen and Franzke (2014). However, long-term TEC trends have not been widely studied. The first study was carried out by Lean et al. (2011), who considered GPS global and regional trends 1995–2010 with the main finding of slow increasing trend ($0.6 \pm 0.3$ TECU decade$^{-1}$, TECU = $10^{16}$ Ne m$^{-2}$) in the daily averaged





GID
5, 385–404, 2015



global TEC-values. One explanation for this trend could be a reduction in the upper atmospheric recombination rates due to cooling in the thermosphere. LEO tomography measurements can have a crucial role in refining the result of Lean et al. (2011) at high latitudes where GPS measurements have accuracy problems due to oblique signal paths.

This paper is organized as follows: In Sect. 2 the SGO ionospheric tomographic data and the ionospheric VTEC estimation are overviewed. Section 3 includes a discussion of the estimated VTEC and IRI-2012 model results. Section 4 concludes the study and provides some notes for future research.

## 2 Data and methodology

The ionospheric tomography reconstructions provided by SGO are solved in two-dimensional latitude-altitude domain. The measurement geometry then resembles the schematic plot in Fig. 3. Figure 4 shows an example result sheet for one overflight from SGO's tomography web archive[1].

The inclination of COSMOS satellites is ~ 83°, i.e. compared to strictly polar orbit, the direction of the satellites is tilted slightly eastwards. The SGO receivers are installed along the inclination angle so that the descending overflights are somewhat parallel to the chain. Figure 1 illustrates how in an optimal case the descending satellite trajectory is aligned with the chain, but also how the ascending overflights are almost perpendicular to the chain. As in two-dimensional ionospheric tomography the longitudinal gradients cannot be taken into account, the set of reconstructions is limited to descending overflights with maximum elevation angles over 60°, when observed from Kokkola station. To get an idea of the trajectories included in analysis, two extremes of descending overflights with maximum elevation angles close to 60° are shown in Fig. 1. Limiting the original data of 66 000 overflights with these criteria results with

[1] http://www.sgo.fi/Data/Tomography/tomoArchive.php





GID
5, 385–404, 2015



a data set of around 10 000 tomographic reconstructions. In Fig. 2 the number of satellite overflights are plotted against satellite elevation. Instead of analyzing complete two-dimensional reconstructions the data is simplified to ionospheric VTEC measurements. The VTEC is obtained by integrating the reconstructed electron densities above each SGO receiver from ground level to satellite altitude. The orbital altitude of COSMOS satellites is approximately 1000 km. The geographical locations of the stations are Nurmijärvi (60.51° N, 24.65° E), Kokkola (63.83° N, 23.16° E), Luleå (65.62° N, 22.14° E), Kiruna (67.85° N, 20.41° E) and Kilpisjärvi (69.02° N, 20.86° E). At the beginning of the observation period, a station in the EISCAT site in Tromsø, Norway, was used, but this station was moved rather soon to Kilpisjärvi. The Nurmijärvi measurements start from June 2004. The reference datasets of IRI-2012[2], F10.7 and sunspot[3] number values are all collected with the same time axis as the tomographic VTEC data. The IRI-2012 VTEC values are integrated from the model results similarly to the tomographic VTEC.

## 3 Results and discussion

To characterize the data, it is first presented as averaged VTEC values in magnetic latitude and magnetic local time (MLT) coordinate system. This is done separately for the complete and seasonal datasets from summer, equinox and winter. In Figs. 5–8 first the data for tomographic then for IRI-2012 VTEC values are shown. Third image illustrates the differences between these two.

The relative diurnal behavior between the data sources is visibly comparable. Both approaches show in dayside VTEC values dawn-dusk asymmetry with higher values in the dusk side. This asymmetry is pronounced particularly during summer time, when according to IRI-2012 enhanced VTEC values extend to pre-midnight hours. In tomography results a similar trend is visible but the extension of high VTEC to night time hours

[2]http://omniweb.gsfc.nasa.gov/vitmo/iri2012_vitmo.html

[3]http://omniweb.gsfc.nasa.gov/form/dx1.html





GID
5, 385–404, 2015



beyond 18 MLT is missing. Both tomography and IRI-2012 show lowest VTEC values in the post-midnight and early morning sectors. At magnetic local daytime the difference in absolute values seems systematic as the estimates from IRI-2012 are close to 5 TECU higher compared to corresponding tomographic VTEC estimates at every season. At the magnetic local night time the differences are in general somewhat smaller and to both directions. At equinox and winter, especially at the higher latitudes, the tomographic VTEC values are higher than the corresponding values from the IRI-2012 model. This difference is likely associated with auroral activity at Kiruna and Kilpisjärvi stations.

In order to deduce whether the solar cycle can be observed from the data, in Figs. 9 and 10 the datasets for the location of Kokkola station are presented as time series for the complete period of 2003–2014. Kokkola is chosen as the representative case as it is located close to the centre of the tomographic domain and also provides good operational coverage in the observation period. Furthermore, in illustrations of this kind, the differences between the values from different stations are almost indistinguishable.

In Fig. 9 the VTEC over Kokkola station is presented as monthly means for each MLT hour. This is done for the whole observation period. In the same figure are presented again the corresponding VTEC values from IRI-2012 model and the differences between them. First of all, Fig. 9 shows the nature of satellite availability. The period of COSMOS satellites is 105 min, which produces a drift in daily times of overflights. The images also show maxima of VTEC in 2003 and in 2014. Similarly to Figs. 5–8 the systematic differences between tomographic and IRI-2012 VTEC values are visible. IRI-2012 VTEC values are on average approximately 40 % higher than tomographic VTEC. A discernible exception from this general trend is in the MLT hours around midnight of year 2003 (blue pixels in the lowest panel of Fig. 9), which is known to be a year of particularly strong space weather activity (see e.g. Juusola et al., 2015).

In Fig. 10, in addition to IRI-2012, the tomographic data are compared to daily sunspot number and F10.7 solar flux index. Here only the midday 11–13 MLT VTEC from Kokkola station and corresponding values from IRI-2012 model were selected for





GID
5, 385–404, 2015



the analysis. Due to a low number of satellites the measurement times are not uniformly represented, i.e. some time slots are over-presented in the data. However, even despite of non-uniformity of the data, the solar cycle dependence is clear. The pattern of tomographic VTEC correspond essentially to reference data.

## 4 Conclusions

In this paper, the SGO's LEO-satellite ionospheric tomography dataset from the period of 2003–2014 is presented. This dataset covers approximately one solar cycle. The primary aim in this paper has been to see the solar cycle effect in the data. For this purpose, the estimated VTEC values were used, which clearly exhibit solar cycle dependent features.

The estimated VTEC values have been compared against the IRI-2012 model. The tomographic VTEC values have a relative agreement with the corresponding VTEC values obtained from the IRI-2012 model, but there is a systematic error between the two. The values based on the IRI-2012 model are on average 40 % higher of those of the tomographic results. Further studies are needed to resolve the reason for this discrepancy.

We suggest that the VTEC values from beacon-based tomographic inversion can constitute a viable tool for studying long-term trends in the atmosphere. The standard long-term trend is usually studied via the F2-layer peak. But as this is a point value, the overall VTEC can import some extra information to the analysis. However, as the data consists only one solar cycle, it is practically impossible to say anything about the long-term trends merely on the basis of the measured VTEC values. Hence, at least one extra cycle for a proper long-term VTEC trend analysis is required.





GID
5, 385–404, 2015



*Acknowledgements.* This work has been funded by European Regional Development Fund (Regional Council of Lapland, decision number A70179), Academy of Finland (decision number 287679) and European Research Council (ERC advanced grant 267700 – Inverse problems). Ionospheric tomography measurements and analyzed data products used in this paper are freely available upon request from Sodankylä Geophysical Observatory.

## References

Austen, J. R., Franke, S. J., and Liu, C. H.: Ionospheric imaging using computerized tomography, Radio Sci., 3, 299–307, 1988. 386

Bilitza, D., Altadill, D., Zhang, Y., Mertens, C., Truhlik, V., Richards, P., McKinnell, L.-A., and Reinisch, B.: The international reference ionosphere 2012 – model of international collaboration, J. Space Weather Space Clim., 4, A07, doi:10.1051/swsc/2014004, 2014. 388

Bremer, J.: Ionospheric trends in mid-latitudes as a possible indicator of the atmospheric greenhouse effect, J. Atmos. Terr. Phys., 54, 1505–1511, 1992. 388

Bremer, J.: Trends in the ionospheric E and F regions over Europe, Ann. Geophys., 16, 986–996, doi:10.1007/s00585-998-0986-9, 1998. 388

Bust, G. S. and Mitchell, C. N.: History, current state, and future directions of ionospheric imaging, Rev. Geophys., 46, RG1003, doi:10.1029/2006RG000212, 2008. 387

Cnossen, I. and Franzke, C.: The role of the Sun in long-term change in the F2 peak ionosphere: new insights from EEMD and numerical modeling, J. Geophys. Res.-Space, 119, 8610–8623, 2014. 388

Jee, G., Lee, H.-B., Solomon, S. C., Cnossen, I., and Franzke, C.: Global ionospheric total electron contents (TECs) during the last two solar minimum periods, J. Geophys. Res.-Space, 119, 2090–2100, doi:10.1002/2013JA019407, 2014. 388

Juusola, L., Viljanen, A., Van De Kamp, M., Tanskanen, E. I., Vanhamäki, H., Partamies, N., and Kauristie, K.: High-latitude ionospheric equivalent currents during strong space storms: regional perspective, Space Weather, 13, 49–60, doi:10.1002/2014SW001139, 2015. 391

Kunitsyn, V. E. and Tereshchenko, E. D.: Ionospheric Tomography, Springer-Verlag, Berlin, Germany, 2003. 387

Lastovicka, J.: Are trends in total electron content (TEC) really positive?, J. Geophys. Res.-Space, 118, 3831–3835, 2013.





GID

5, 385–404, 2015



Lean, J. L., Emmert, J. T., Picone, J. M., and Meier, R. R.: Global and regional trends in ionospheric total electron content, J. Geophys. Res.-Space, 116, A00H04, doi:10.1029/2010JA016378, 2011. 388

Markkanen, M., Lehtinen, M., Nygrén, T., Pirttilä, J., Helenius, P., Vilenius, E., Tereshchenko, E. D., and Khudukon, B. Z.: Bayesian approach to satellite radiotomography with applications in the Scandinavian sector, Ann. Geophys., 13, 1277–1287, 1995, http://www.ann-geophys.net/13/1277/1995/. 387

Norberg, J., Roininen, L., Vierinen, J., Amm, O., McKay-Bukowski, D., and Lehtinen, M.: Ionospheric tomography in Bayesian framework with Gaussian Markov random field priors, Radio Sci., 50, 138–152, doi:10.1002/2014RS005434, 2015. 387

Nygrén, T., Markkanen, M., Lehtinen, M., Tereshchenko, E. D., Khudukon, B. Z., Evstafiev, O. V., and Pollari, P.: Comparison of F-region electron density observations by satellite radio tomography and incoherent scatter methods, Ann. Geophys., 14, 1422–1428, doi:10.1007/s00585-996-1422-7, 1996. 387

Roble, R. G. and Dickinson, R. E.: How will changes in carbon dioxide and methane modify the mean structure of the mesosphere and thermosphere, Geophys. Res. Lett., 16, 1441–1444, doi:10.1029/GL016i012p01441, 1989. 388

Ulich, T. and Turunen, E.: Evidence for long-term cooling of the upper atmosphere in ionosonde data, Geophys. Res. Lett., 24, 1103–1106, 1997. 388

Upadhyay, H. O. and Mahajan, K. K.: Atmospheric greenhouse effect and ionospheric trends, Geophys. Res. Lett., 25, 3375–3378, 1998. 388

Vierinen, J., Norberg, J., Lehtinen, M. S., Amm, O., Roininen, L., Väänänen, A., Erickson, P. J., and McKay-Bukowski, D.: Beacon satellite receiver for ionospheric tomography, Radio Sci., 49, 1141–1152, doi:10.1002/2014RS005431, 2014. 387





GID
5, 385–404, 2015



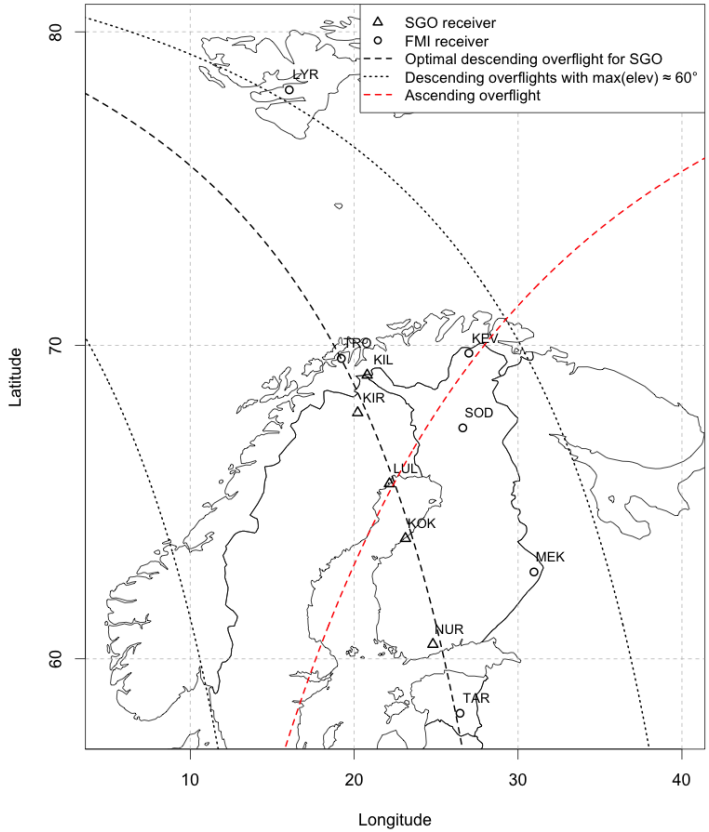


**Figure 1.** Current locations of SGO and FMI tomography chains.





GID
5, 385–404, 2015

Sodankylä ionospheric tomography dataset 2003–2014

J. Norberg et al.



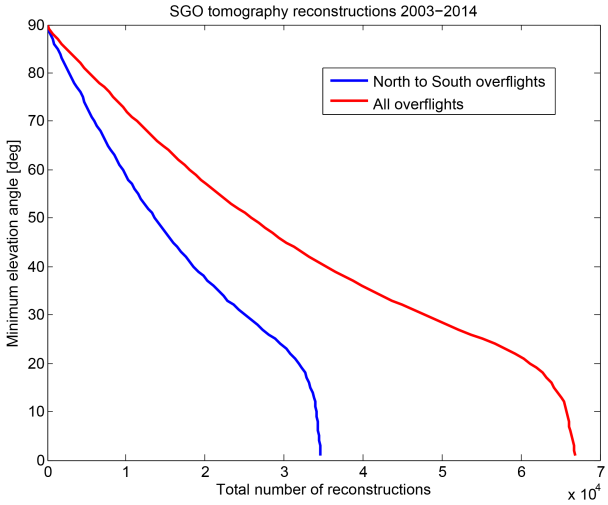


**Figure 2.** The number of satellite overflights over the whole observation period with respect to minimum threshold elevation.





GID
5, 385–404, 2015



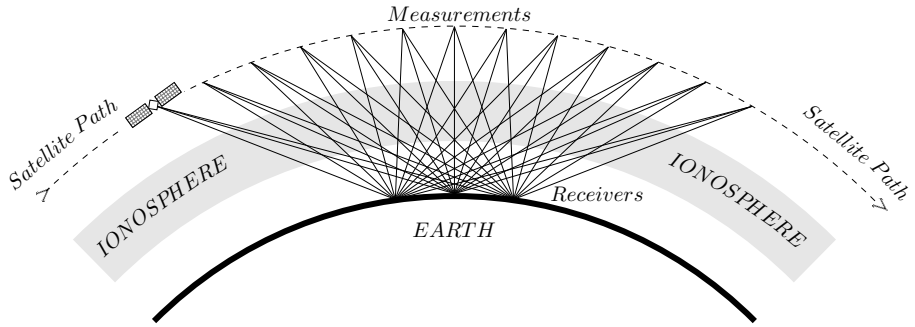


**Figure 3.** Schematic plot of ionospheric tomography with LEO beacon satellites.





GID
5, 385–404, 2015



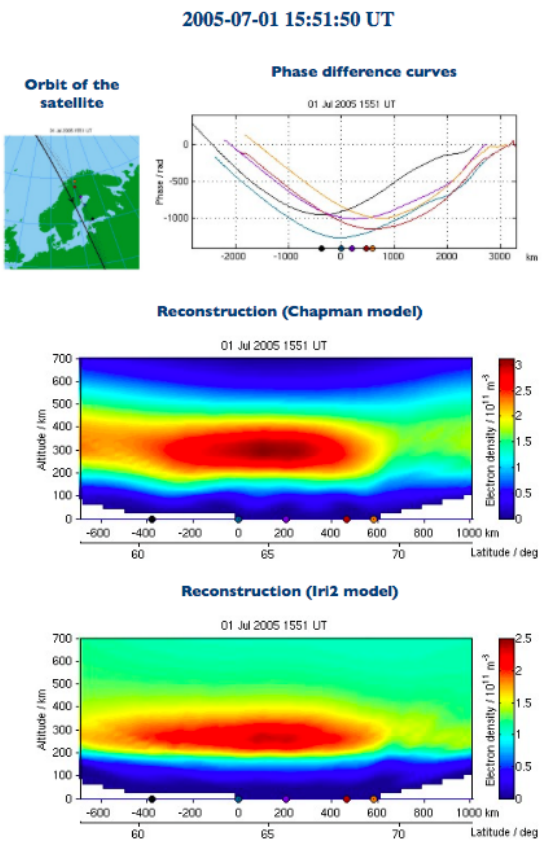


**Figure 4.** Tomographic reconstruction result from Sodankylä Geophysical Observatory. The satellite trajectory, observed phase difference curves and tomographic results with two different prior models. The receiver stations are shown as coloured points. The origin of the km axis is placed to Kokkola station.





GID
5, 385–404, 2015



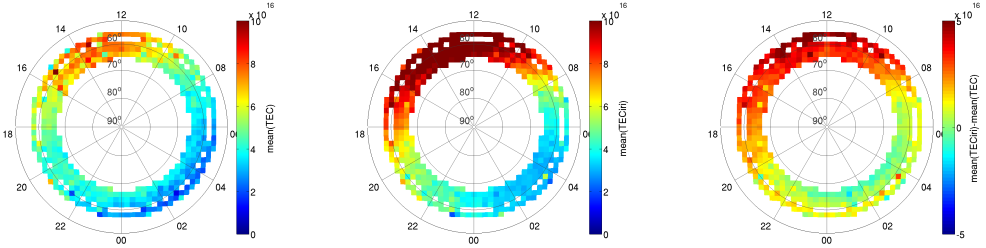


**Figure 5.** Magnetic local time mean values for tomographic VTEC, corresponding IRI-2012 values and the difference between the two.





GID
5, 385–404, 2015



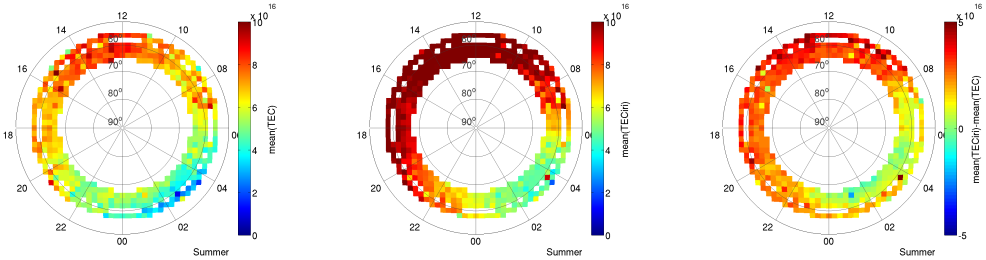


**Figure 6.** Magnetic local time mean values for summer time tomographic VTEC, corresponding IRI-2012 values and the difference between the two.





GID
5, 385–404, 2015



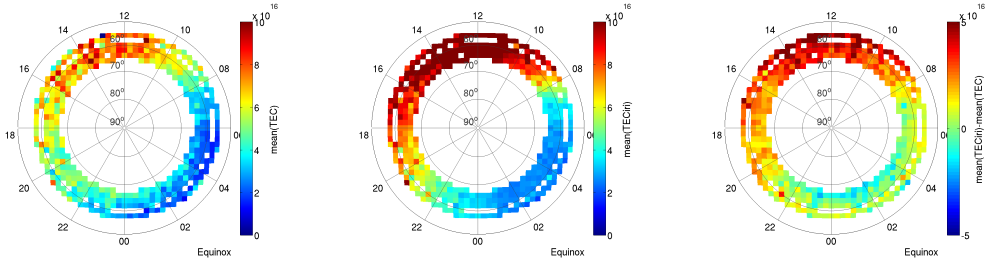


**Figure 7.** Magnetic local time mean values for equinox time tomographic VTEC, corresponding IRI-2012 values and the difference between the two.





GID
5, 385–404, 2015



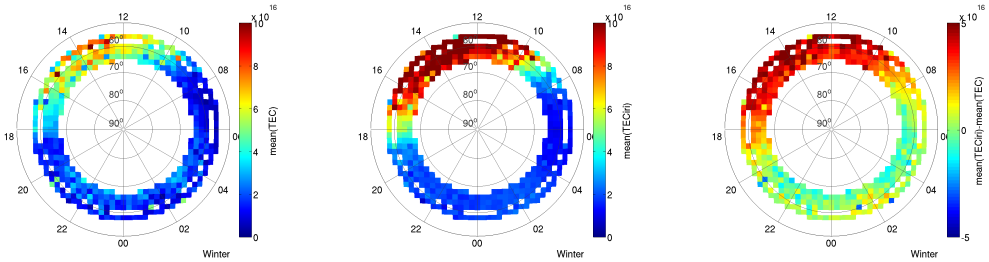


**Figure 8.** Magnetic local time mean values for winter time tomographic VTEC, corresponding IRI-2012 values and the difference between the two.





GID
5, 385–404, 2015



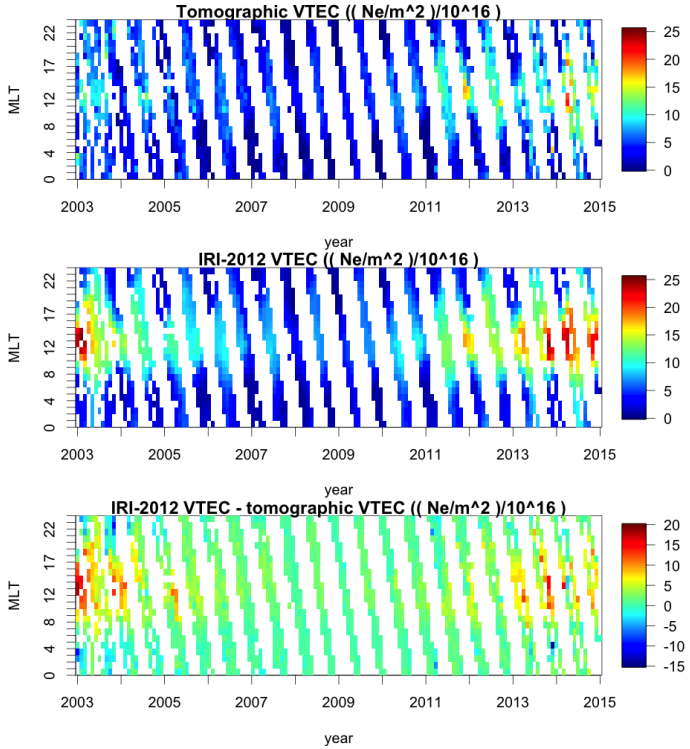


**Figure 9.** Monthly VTEC averages for each MLT hour over Kokkola station.





GID
5, 385–404, 2015

Sodankylä ionospheric tomography dataset 2003–2014

J. Norberg et al.



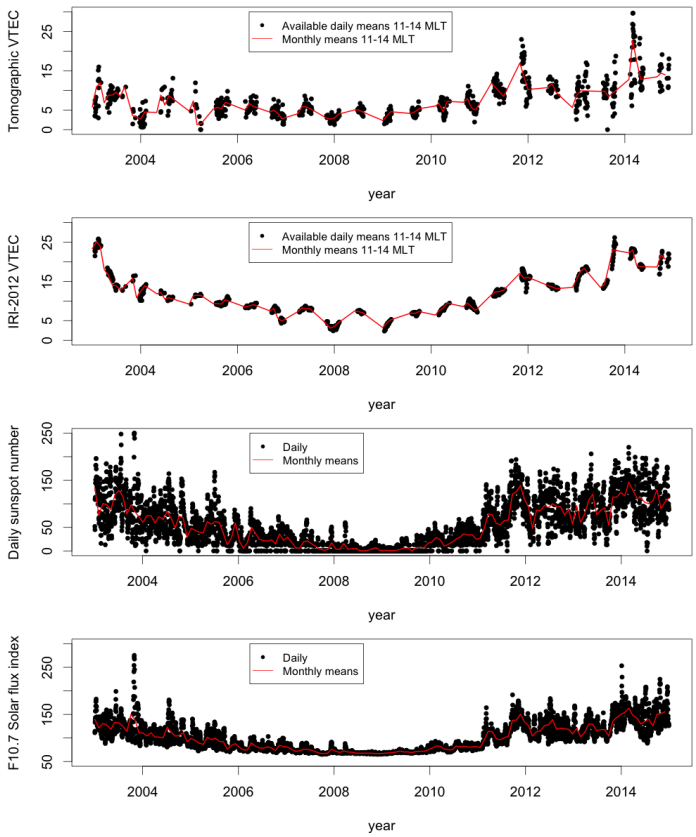


**Figure 10.** VTEC values over Kokkola averaged from 11–14 MLT vs. corresponding IRI-2012 model values, sunspot number and solar flux index F10.7.





GID
5, 385–404, 2015